



ORIGINAL ARTICLE

A facile synthesis of 1,3,4-oxadiazole-based carbamothioate molecules: Antiseizure potential, EEG evaluation and *in-silico* docking studies



Nasir Rasool^a, Zainib Razzaq^a, Samreen Gul Khan^{a,*}, Sana Javaid^b,
Naheed Akhtar^c, Sadaf Mahmood^a, Jørn B. Christensen^d, Ataf Ali Altaf^e,
Syed Muhammad Muneeb Anjum^f, Faleh Alqahtani^g, Abdullah F. AlAsmari^g,
Imran Imran^{b,*}

^a Department of Chemistry, Government College University, Faisalabad 38000, Pakistan

^b Department of Pharmacology, Faculty of Pharmacy, Bahauddin Zakariya University, 60800 Multan, Pakistan

^c Department of Biochemistry, Government College University Faisalabad, Faisalabad 38000, Pakistan

^d Department of Chemistry, Faculty of Science, University of Copenhagen, Copenhagen, Denmark

^e Department of Chemistry, University of Okara, Okara 56300, Pakistan

^f The Institute of Pharmaceutical Sciences, University of Veterinary & Animal Sciences, Lahore, Pakistan

^g Department of Pharmacology and Toxicology, College of Pharmacy, King Saud University, Riyadh 11451, Saudi Arabia

Received 10 August 2022; accepted 18 January 2023

Available online 24 January 2023

KEYWORDS

Epilepsy;
6 Hz;
PTZ;
1,3,4-oxadiazole;
Electroencephalogram;
Seizure

Abstract In present work, a series of novel structural hybrids of 1,3,4-oxadiazole and carbamothioate was designed by chemical modification of 2-(4-isobutylphenyl)propanoic acid. Target compounds (**7a-f**) were synthesized in significant yields (84–88 %) by coupling compound (**4**) with different electrophiles under different reaction conditions. The structures of oxadiazole based carbamothioate derivatives were confirmed by spectroscopic (FTIR, ¹H NMR, ¹³C NMR) and physicochemical methods. During *in-vivo* experimentation, all synthesized compounds were tested through 6 Hz (32 mA) and PTZ (80 mg/kg) mouse seizure models. The **7b** and **7c** showed significant outcomes ($P < 0.05$) in terms of seizure severity, protection and mortality. The behavioural outcomes of PTZ tests were further strengthened with video-electroencephalogram (vEEG) findings in which EEGs were analyzed for epileptic spikes to understand the impact of **7b** and **7c** treatment on these ictal activities. The **7b** was found most efficient in reducing the seizure spiking activity in

* Corresponding authors.

E-mail addresses: samreengul@gcuf.edu.pk (S. Gul Khan), Imran.ch@bzu.edu.pk (I. Imran).

Peer review under responsibility of King Saud University.



brains of PTZ-treated mice while both **7b** and **7c** significantly reduced overall PTZ-induced seizure severity. The molecular docking studies also predicted the BBB permeability, reduced binding energies and good compound interaction with GABA_A receptors and SV2A protein. Therefore, the observed pharmacological outcomes might be attributed to the GABA_A agonistic and SV2A modulating potential of these oxadiazole-carbamothioate hybrid compounds.

© 2023 The Author(s). Published by Elsevier B.V. on behalf of King Saud University. This is an open access article under the CC BY license (<http://creativecommons.org/licenses/by/4.0/>).

1. Introduction

More than 70 million of world's population is suffering from epilepsy (Löscher et al., 2020). Uncontrolled epilepsy or failure to attain seizure control with standard anticonvulsant medications is intricately associated with pharmacoresistant epilepsy (Sharma et al., 2015). Drug resistance epilepsy (DRE) is not only responsible for the intractable seizures but also causes neurobiochemical changes in the brain leading to neuropsychiatric dysfunctions, life-long dependency and disease-induced socioeconomic burden (Kwan and Brodie, 2002). A systematic review has recently reported that the overall prevalence and incidence of DRE have elevated from 0.11 to 0.58 % and 0.06 to 0.51 %, respectively (Fattorusso et al., 2021).

The quality of life for epileptic patients is improved by prescribing conventional therapeutic choices. However, their utilization is associated with idiosyncratic dose-related toxicity and addictive potential (Zaccara et al., 2007). Additionally, pharmacoresistant epilepsy necessitates the development of appropriate novel therapeutic options. Currently available antiseizure drugs are effective in preventing epileptogenesis and convulsions in <80 % of epileptic patients (Perucca, 2021). Furthermore, the extended use of antiepileptic drugs is related to unwanted adverse effects that might prove life-threatening (Obniska et al., 2012). Due to the aforementioned reasons, scientists are continuously attempting to synthesize new chemical agents of antiepileptic potential with better safety profiles.

The screening of novel compounds for anticonvulsant potential relies profoundly on the established preclinical animal models of epileptic seizures. Generally, experimental seizure induction involves electrical and/or chemical stimulation of the rodent brain (Löscher, 1999). The 6-Hertz (6 Hz) and pentylenetetrazole (PTZ)-induced seizure models are broadly used in the initial screening of antiepileptic compounds (Löscher, 2011). The 6 Hz model utilizes the corneal application of different current intensities (22, 32 or 44 mA) to identify the new compounds with antiseizure potential. However, at high stimulation intensities i.e. 44 mA, most of the AEDs lose their efficacy so it can be used to identify new compounds that can be employed in the treatment of refractory partial epilepsy (Barton et al., 2001).

Molecular hybridization is a simple and effective tool to covalently combine multiple drug pharmacophores. Our ongoing research focuses on design and synthesis of pharmacologically active diverse polyvalent scaffolds as anticonvulsant agent. 1,3,4-oxadiazole is reported to have versatile nature and great importance in medicinal chemistry such as anticonvulsant agents (Almasirad et al., 2014; Zarghi and Arfaei, 2011), anticancer (Yadav et al., 2017), antifungal (Karaburun et al., 2019), antioxidant (Abd-Elzaher et al.,

2016), anti-inflammatory (Chawla et al., 2018, Gulnaz et al., 2019), antibacterial (Zheng et al., 2018), anti-HIV (Akhtar et al., 2007; Khan et al., 2016) antimicrobial ((Bala et al., 2014)), antitumor (Mansouri et al., 2021), antipyretic (Xu et al., 2018) as well as pyrophosphatases and phosphodiesterases (Akhtar et al., 2007). Carboxamide is reported to be significantly important pharmacophore of antiepileptic drugs like levetiracetam, carbamazepine, and brivaracetam (Ahmad et al., 2019). On this basis, we have designed a hybrid of oxadiazole and carbamothioate pharmacophore together in one molecule to prevent the progression of epilepsy. We selected 2-(4-isobutylphenyl) propanoic acid core for chemical derivatization. Our designed molecular framework contains hydrophobic aryl rings on each side of oxadiazole and carbamothioate. In the current study, the synthesized oxadiazole-carbamothioate derivatives **7a**, **7b**, **7c**, **7d**, **7e** and **7f** were preliminarily tested for antiseizure potential through 6 Hz (32 mA) and PTZ (80 mg/kg) mouse models. This study aimed to further authenticate the antiseizure potential of potent compounds by examining their effects on electroencephalogram (EEG) activity in the PTZ model. The effects of compounds were evaluated for epileptic spikes analysis to examine whether these ictal activities in EEG are affected by test compounds. For further understanding of observed outcomes, the binding energies and interactions of compounds were predicted with target molecular receptors.

2. Chemistry and experimental details

2.1. Chemistry

Melting points of all derivatives were checked using open capillary tube methods and an electrical melting point (Stuart SMP10 melting point apparatus). 2-(4-isobutylphenyl) propanoic acid was used as a starting material. Infrared spectra were obtained using potassium bromide discs on an FT-IR spectrophotometer (BRUKER) with a wavelength range of 4000–400 cm⁻¹ and expressed in wave number (cm⁻¹) at GC University's Hi Tech Lab. ¹H NMR and ¹³C NMR spectra were carried out in deuterated solvent i.e. the exchangeable protons were exchanged by D₂O. DMSO-d₆ on Avance Bruker using 500 MHz spectrophotometer (¹H NMR) and 75 MHz to 100 MHz (¹³C NMR) NMR spectrophotometer at Department of Chemistry, University of Copenhagen, Denmark. The chemical shift was expressed in δ ppm. Reaction progress and completion was monitored by TLC.

2.1.1. Synthesis of methyl 2-(4-isobutylphenyl)propanoate (2)

Dry methanol (30–35 ml) was added into ibuprofen (1) (6.g, 0.02 mol) in a round bottom flask. Conc. H₂SO₄ (2.5 ml) was added into the flask containing methanol and ibuprofen.

The reaction was set to reflux for 6 to 7 h. The reaction completion was checked using thin layer chromatographic technique. After successful completion, the solvent was removed by evaporation. Distilled water was added into the crude product and ester was extracted using solvent extraction technique. Diethyl ether was used for extraction of ester. Sodium carbonate solution was then added into ester containing layer. The ester was washed and dried over anhydrous sodium carbonate. The product was then concentrated. The compound (2) was obtained as pale-yellow oily liquid; molecular formula $C_{14}H_{20}O_2$; Mol. Wt. 220.15; Yield: (90 %); b.p. 263–265 °C; IR (KBr) cm^{-1} : 1736.34 (C=O stretch (ester)), 1203.37 (C–C–O stretch), 1162.81 (O–C–C stretch); Anal. C, 76.33; H, 9.15; O, 14.52 (supplementary data, S1).

2.1.2. Synthesis of 2-(4-isobutylphenyl)propanehydrazide (3)

2-(4-isobutylphenyl)propanehydrazide was synthesized by dissolving methyl 2-(4-isobutylphenyl)propanoate (2 g, 0.02 mol) in 15 ml methanol (MeOH) was taken in oven dried RBF, then added hydrazine hydrate (2 ml). Then the solution was set to reflux for 10–12 h at to 90–100 °C. After the completion, chilled water was added in reaction to get product. Ibuprofen hydrazide was separated as a white crystalline solid. The spectroscopic and physical date of the 2-(4-isobutylphenyl)propanehydrazide is given as Rf value (*n*-hexane: ethyl acetate 7:3) = 0.83; molecular formula $C_{13}H_{20}N_2O$; Mol. Wt. 220.16; Yield: (88 %); m.p. 77–78 °C; IR (KBr) cm^{-1} : 3272.75, 2963.11, 1640.11, 1604.85, 1466.29, 1366.60, 906.66, 686.81. Mol. Wt. 220.16. Anal. C, 70.87; H, 9.15; N, 12.72; O, 7.26 (supplementary data, S2).

2.1.3. Synthesis of 5-(1-(4-isobutylphenyl)ethyl)-1,3,4-oxadiazole-2-thiol (4)

In an oven dried round bottom flask, 2-(4-isobutylphenyl)propanehydrazide (0.02 mol) was dissolved in methanol (30 ml). KOH (0.02 mol) and CS_2 (0.03 mol) were also added in reaction flask. The mixture was refluxed at 95 °C for 10–11 h. Reaction progress as well as completion was continuously monitored by TLC. After the completion, chilled water was added in flask to get precipitates of product the product. Mixture was acidified with HCl to pH-4.3. Precipitates were filtered and washed with water. The product was also recrystallize using absolute ethanol. 5-(1-(4-isobutylphenyl)ethyl)-1,3,4-oxadiazole-2-thiol was separated as off white crystalline solid having molecular formula $C_{14}H_{18}N_2O_3S$; Mol. Wt. 482.26; Yield: (84 %); m. p. 115–118 °C; IR (KBr) cm^{-1} : 2448.56, 1507.89, 1454.29, 1294.98, 1174.54, 1069.78, 989.93, 736.98. Anal. C, 69.67; H, 9 = 7.84; N, 5.80; O, 9.94; S, 6.64 (supplementary data, S3-S5).

2.1.4. Synthesis of *N*-substituted aryl/alkyl 2-bromocarbamides (6a-f)

In an oven dried round bottom flask, the *N*-substituted aryl/alkyl amines (5a-5f, 12.0 mol) were dissolved in 10.0 ml of 5 % Na_2CO_3 solution. Carbonic dibromide (12.0 mmoles) was introduced gradually into the above reaction mixture. The mixture containing round bottom flask was shaken gently till precipitation. Reaction progress as well as completion was continuously checked by TLC. After the completion, chilled water was added in flask to get precipitates of product the product. Precipitates of the product (6a-f) were filtered and

dried. The product were also recrystallized using absolute ethanol.

2.1.5. Synthesis of *N*-substituted 5-(1-(4-isobutylphenyl)ethyl)-1,3,4-oxadiazole-2-yl-2-sulfanyl carbamide derivatives (7a-f)

Different *N*-substituted 5-(1-(4-isobutylphenyl)ethyl)-1,3,4-oxadiazole-2-yl-2-sulfanyl carbamide derivatives were synthesized in good yield by the stirring 4 with different substituted aralkyl/alkyl/aryl 2-bromocarbamides (6a-f) using DMF and NaH at room temperature. Reaction progress as well as completion was continuously checked by TLC. After the completion, chilled water was added in flask to get precipitates of product. Precipitates of the product were filtered and dried. The product was also recrystallized using absolute ethanol.

2.1.6. *S*-(5-(1-(4-isobutylphenyl)ethyl)-1,3,4-oxadiazol-2-yl)(2,3 dimethylphenyl) carbamothioate (7a)

Off white amorphous solid; (83 %); $C_{23}H_{27}N_3O_2S$; Mol. Wt. 409.55; m.p 157–159 °C; IR (KBr, cm^{-1}) 2906.21, 2363.96, 2313.72, 2164.19, 1680.73, 1515.73, 698.36, 637.52; 1H NMR (500 MHz, DMSO) δ 9.29 (s, 1H, N–H), 7.44–7.42 (d, 1H, $J = 10$, H-6'), 7.20–7.19 (d, 2H, $J = 10$, aromatic-H-9 & aromatic-H-13), 7.15–7.13 (d, 2H, $J = 5$, aromatic-H-10 & aromatic-H-12), 7.06–7.03 (t, 1H, $J = 5$ & 10, aromatic-H-5'), 6.94–6.92 (d, 1H, $J = 10$, aromatic -H-4'), 4.32–4.28 (q, 1H, aromatic-H-6), 2.43–2.41 (d, 1H, $J = 5$ CH₂-14), 2.23 (s, 3H, CH₃-2') 2.07 (s, 3H, CH₃-3'), 1.84–1.79 (m, 1H, H-15) 1.59–1.58 (d, $J = 5$, 3H, CH₃-7), 0.86–0.85 (d, $J = 5$ Hz, 6H, H-16, H-17). ^{13}C NMR (126 MHz, DMSO) 162.15(C, C=O), 161.37(C, C5), 139.98(C, C-11), 138.41 (2C, C-3' & C-8), 137.06(C-3'), 136.63(C-1'), 129.26(C-10 & C-12), 128.09(C-2'), 126.85(C-9 & C-13), 125.51(C-4' & C-5'), 119.40(C-6), 44.18(CH₂, C-14), 36.06(C-6), 29.40(C-15), 22.13 (2CH₃, C-16 & C-17), 20.19(CH₃, C-7), 19.38(CH₃, C-3'), 13.75(CH₃, C-2'); EIMS *m/z*: 409.18 (100.0 %), 410.19 (24.9 %), 411.18 (4.5 %), 411.19 (2.7 %), 412.18 (1.1 %), 410.18 (1.1 %); Elemental Analysis: C, 67.45; H, 6.65; N, 10.26; O, 7.81; S, 7.83 (supplementary data, S6-S9).

2.1.7. *S*-(5-(1-(4-isobutylphenyl)ethyl)-1,3,4-oxadiazol-2-yl)(4methoxyphenyl) carbamothioate (7b)

Off white amorphous solid; (80 %); $C_{22}H_{25}N_3O_3S$; Mol. Wt. 411.52; m.p 145–147 °C; IR (KBr, cm^{-1}) 2906.21 (C–H), 2363.96 (C–O), 2313.72 (C=C), 2164.19 (C=C), 1515.73 (C=O ring), 698.36 (C–H), 679.66 (C–H), 666.02 (C–O–C), 651.67 (C=C), 637.52 (C–H). 1H NMR (500 MHz, DMSO) δ 10.10 (s, 1H, N–H), 7.43–7.41, (d, 2H, $J = 10$ Ar H-2' & H-6'), 7.21–7.19 (d, 2H, $J = 10$ aromatic-H-9 & aromatic-H-13), 7.15–7.13 (d, 2H, $J = 10$, aromatic-H-10 & aromatic-H-12), 6.91–6.89 (d, 2H, $J = 10$, aromatic-H-3' & aromatic-H-5'), 4.34–4.29 (q, 1H, H-6), 3.71 (s, 3H, OCH₃-4'), 2.43–2.41 (d, 2H, $J = 10$ CH₂-14), 1.82–1.78 (m, 1H, H-15) 1.60 (d, $J = 5$, 3H, CH₃-7), 0.86–0.84 (d, $J = 10$ Hz, 6H, H-16 & H-17). ^{13}C NMR (126 MHz, DMSO) 161.39, (C=O), 159.98.17(C5), 153.83(C-4'), 140.15(C11), 138.24(C-8), 131.80(C-10 & C-12), 129.53(C-1), 126.53(C-9 & C-13) 117.82(C-2' & C-6'), 113.93(C-3' & C-5'), 55.31(CH₃, OCH₃-4'), 43.19(CH₂, C-14), 36.06(1C, C-6), 29.67(1CH, C-15) 21.86 (2C, CH₃-1 & CH₃-17), 19.38(1C, CH₃-7). EIMS *m/z*: 411.16 (100.0 %), 412.17 (23.8 %), 413.16 (4.5 %), 413.17 (2.7 %), 412.16 (1.1 %), 414.16 (1.1 %); Elemental Analysis: C,

64.21; H, 6.12; N, 10.21; O, 11.66; S, 7.79 (supplementary data, S10-S13).

2.1.8. *S*-(5-(1-(4-isobutylphenyl)ethyl)-1,3,4-oxadiazol-2-yl) (4-ethoxyphenyl)carbamothioate (7c)

Off white amorphous solid; (85 %); $C_{23}H_{27}N_3O_3S$; Mol. Wt. 425.55; m.p 137–139 °C; IR (KBr, cm^{-1}) 3734.81, 2363.60, 2312.63, 2164.57, 2121.33, 2034.35, 1981.56, 1965.41, 1949.75, 1938.69, 1695.15, 1516.80, 641.28; 1H NMR (400 MHz, $CDCl_3$) 7.27–7.25 (d, 2H, $J = 8$, aromatic-H-2' & aromatic-H-6'), 7.18–7.16 (d, 2H, $J = 8$ aromatic-H-9 & aromatic-H-13), 7.11–7.09 (d, 2H, $J = 8$ aromatic-H-10 & aromatic-H-12), 6.83–6.81 (d, 2H, $J = 8$, aromatic-H-3' & aromatic-H-5') 4.23–4.17 (q, 1H, H-6), 3.98–3.97 (d, 2H, OCH_2 -4'), 2.44–2.42 (d, 2H, $J = 8$ CH_2 -14), 1.86–1.77 (m, 1H, H-15) 1.69 (d, $J = 8$, 3H, CH_3 -7), 1.39–1.36 (t, 3H, OCH_2 - CH_3 -4'), 0.88–0.86 (d, $J = 8$ Hz, 6H, H-16 & H-17) (supplementary data, S14-S16). ^{13}C NMR (126 MHz, DMSO) 161.85(C, C=O), 160.01(C, C5), 153.49(C, C-4'), 140.13(C, C11), 138.45(C, C-8), 131.85(C-10 & C-12), 129.26(C, C-1), 126.84(C-9 & C-13) 118.13(C-2' & C-6'), 114.76(C-3' & C-5'), 63.15($1CH_2$, OCH_2 -4'), 44.19(CH_2 , C-14), 36.01(1C, C-6), 29.74($1CH_3$, C-15) 22.23(2C, CH_3 -1 & CH_3 -17), 19.38(1C, CH_3 -7), 14.82(OC_2H_5 , CH_3 -4'); EIMS m/z : 425.18 (100.0 %), 426.18 (24.9 %), 427.17 (4.5 %), 427.18 (3.0 %), 428.18 (1.1 %), 426.17 (1.1 %); Elemental Analysis: C, 64.92; H, 6.40; N, 9.87; O, 11.28; S, 7.53 (Fig. 1).

2.1.9. *S*-(5-(1-(4-isobutylphenyl)ethyl)-1,3,4-oxadiazol-2-yl) (2-methylphenyl)carbamothioate (7d)

Off white amorphous solid; (86 %); $C_{22}H_{25}N_3O_2S$; Mol. Wt. 395.52; m.p 191–193 °C; IR (KBr, cm^{-1}) 2906.21, 2363.96, 2313.72, 2164.19, 1690.15, 1515.73, 698.36; 1H NMR (500 MHz, DMSO) δ 9.32 (s, 1H, N–H), 7.74–7.72 (d, 1H, $J = 10$, H-3'), 7.21–7.20 (d, 2H, $J = 5$, aromatic-H-9 & aromatic-H-13), 7.17–7.15 (d, 2H, $J = 10$, aromatic-H-10 & aromatic-H-12), 7.15 (d, 1H, $J = 5$ & 10, aromatic-H-6'), 7.14 (t, 1H, aromatic-H-5'), 6.99–6.97 (t, 1H, $J = 5$, aromatic-H-4'), 4.34–4.30 (q, 1H, H-6), 2.43–2.42 (d, 1H, $J = 5$ CH_2 -14), 2.22 (s, 3H, CH_3 -2') 1.84–1.77 (m, 1H, H-15) 1.61–1.59 (d, $J = 5$, 3H, CH_3 -7), 0.86–0.85 (d, $J = 5$ Hz, 6H, H-16, H-17). ^{13}C NMR (126 MHz, DMSO) 162.21(C=O), 160.92(C5), 139.90(C-11), 138.51 (C-8), 136.80 (C-1'), 130.49(C-2'), 129.11(C-3'), 128.24(C-10 & C-12), 126.85(C-4'), 126.35(C-9 & C-13), 123.29(C-5'), 120.17(C-6'), 43.89(CH_2 , C-14), 36.63(C-6), 29.41(C-15), 22.44(2 CH_3 , C-16 & C-17), 19.41(CH_3 , C-7), 17.99(CH_3 , C-2'); EIMS m/z : 395.17 (100.0 %), 396.17 (23.8 %), 397.16 (4.5 %), 397.17 (2.7 %), 396.16 (1.1 %), 398.17 (1.1 %); Elemental Analysis: C, 66.81; H, 6.37; N, 10.62; O, 8.09; S, 8.11 (supplementary data, S17-S21).

2.1.10. *S*-(5-(1-(4-isobutylphenyl)ethyl)-1,3,4-oxadiazol-2-yl) (phenyl)carbamothioate (7e)

Off white amorphous solid; (84 %) $C_{21}H_{23}N_3O_2S$; Mol. Wt. 381.49; m.p 133–135 °C; IR (KBr, cm^{-1}) 3666.46, 2346.03,

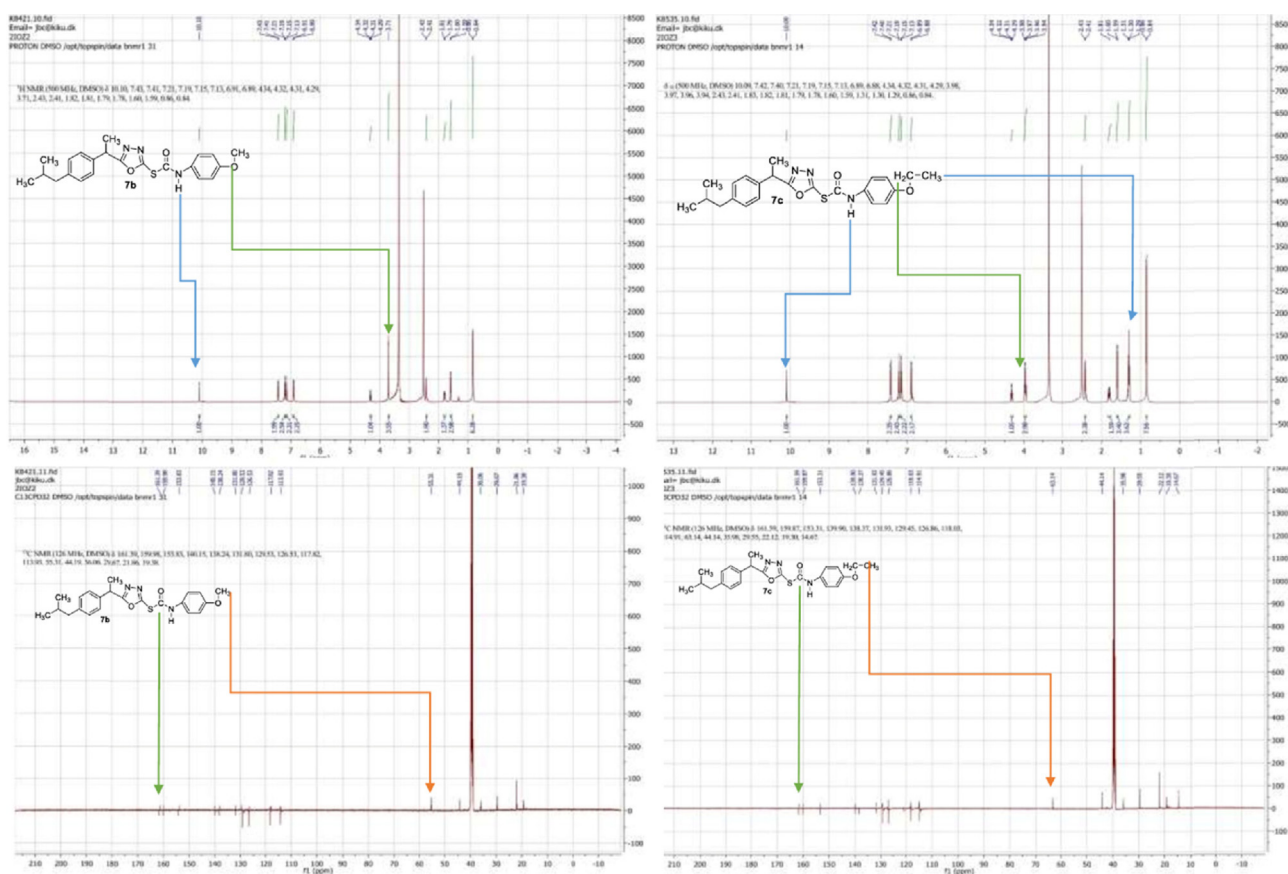


Fig. 1 1H NMR and ^{13}C NMR spectra of **7b** and **7c**.

2313.66, 2160.86, 2120.94, 2023.86, 2008.29, 1695.15, 1618.61, 1562.64, 1540.63 1445.89; ¹H NMR (500 MHz, DMSO) δ 9.32 (s, 1H, N—H), 7.52–7.50 (d, 2H, *J* = 10, aromatic-H-2' & aromatic-H-6'), 7.32–7.30 (t, 2H, *J* = 5, aromatic-H-3' & aromatic-H-5'), 7.21–7.20 (d, 2H, *J* = 5, aromatic-H-9 & aromatic-H-13), 7.15–7.13 (d, 2H, *J* = 10, aromatic-H-10 & aromatic-H-12), 6.98–6.95 (t, 1H, *J* = 5, aromatic-H-4'), 4.36–4.33 (q, 1H, H-6), 2.42–2.41 (d, 1H, *J* = 5 CH₂-14), 1.83–1.79 (m, 1H, H-15) 1.61–1.60 (d, *J* = 5, 3H, CH₃-7), 0.86–0.85 (d, *J* = 5 Hz, 6H, H-16, H-17). ¹³C NMR (126 MHz, DMSO) 161.96(C=O), 159.98(C5), 140.10(C-11), 138.71 (C-8), 138.32(C-1'), 129.28(C-3' & C-5') 128.95(C-10 & C-12), 126.86(C-4'), 126.86(C-9 & C-13), 121.44(C-4'), 116.70(C-2 & C-6'), 43.89(CH₂, C-14), 36.08(C-6), 29.40(C-15), 22.16(2CH₃, C-16 & C-17), 19.36(CH₃, C-7); EIMS *m/z*: 381.15 (100.0 %), 382.15 (22.7 %), 383.15 (4.5 %), 383.16 (2.5 %), 382.15 (1.1 %), 384.15 (1.0 %); Elemental Analysis: C, 66.12; H, 6.08; N, 11.01; O, 8.39; S, 8.40 (supplementary data, S22-S23).

2.1.11. *S*-(5-(1-(4-isobutylphenyl)ethyl)-1,3,4-oxadiazol-2-yl) (2-chlorophenyl) carbamothioate (7f)

Off white amorphous solid; (88 %); C₂₁H₂₂ClN₃O₂S Mol. Wt. 415.94; m.p 121–123 °C; IR (KBr, cm⁻¹) 2906.21, 2363.96, 2313.72, 2164.19, 1680.15, 1515.73, 698.36, 679.66; ¹H NMR (500 MHz, DMSO) δ 9.32 (s, 1H, N—H), 7.88 (d, 1H, *J* = 10, aromatic-H-6'), 7.64 (d, 1H, *J* = 10, aromatic-H-3'), 7.40–7.37 (t, 1H, *J* = 5 & 10, aromatic-H-5'), 7.22–7.20 (d, 2H, *J* = 10, aromatic-H-9 & aromatic-H-13), 7.15–7.13 (d, 2H, *J* = 10, aromatic-H-10 & aromatic-H-12), 7.06–7.03 (t, 1H, *J* = 5 & 10, aromatic-H-4'), 4.35–4.32 (q, 1H, H-6), 2.43–2.41 (d, 1H, *J* = 10 CH₂-14), 1.85–1.78 (m, 1H, H-15) 1.60–1.59 (d, *J* = 5, 3H, CH₃-7), 0.86–0.84 (d, *J* = 10 Hz, 6H, H-16, H-17). ¹³C NMR (126 MHz, DMSO) 162.72(C, C=O), 160.11(C5), 139.91(C-11), 138.32 (C-8), 137.00(C-1'), 133.11(C-3'), 129.27(C-10 & C-12), 128.23(C-4'), 127.27(C-9 & C-13), 125.36(C-5'), 123.03(C-6'), 114.89(C-2'), 44.39 (CH₂, C-14), 36.29(C-6), 29.77(C-15), 22.30(2CH₃, C-16 & C-17), 19.42(CH₃, C-7); EIMS *m/z*: 415.11 (100.0 %), 417.11 (32.0 %), 416.12 (22.7 %), 418.11 (7.3 %), 417.11 (4.5 %), 417.12 (2.5 %), 419.10 (1.4 %), 416.11 (1.1 %), 418.11 (1.0 %); Elemental Analysis: C, 60.64; H, 5.33; Cl, 8.52; N, 10.10; O, 7.69; S, 7.71 (supplementary data, S24-S28).

2.2. Screening for antiseizure potential

2.2.1. Animals

The 6–8 weeks old Balb/c mice of both sexes weighing 25–40 g were used in this study. The animals used in this study were obtained from the animal house of the Faculty of Pharmacy, Bahaiddin Zakariya University, Multan. The housing conditions were maintained with 25 °C and 12 h day/night cycle. The animals were given free access to standard rodent food and water. Before experimentation, the animals were habituated to the test environment and experimenter's handling to maximally avoid handling-induced stress. All experimental studies on animals were under the ARRIVE guidelines keeping in view the minimal number of animal usage and permitted by the departmental Ethical Committee vide # 29/SC/2022.

2.2.2. Chemicals and drugs

All synthetic compounds named **7a**, **7b**, **7c**, **7d**, **7e** and **7f** were injected through the intraperitoneal route at a dose of 100 mg/kg. The dilution of each compound was made by dissolving 10 mg of the compound in 1 ml of 1 % tween 80 just before administration. The levetiracetam (50 mg/kg) (Nieoczym et al., 2013) and diazepam (5 mg/kg) (Ahmad et al., 2019) were dissolved in distilled water and injected intraperitoneally.

2.2.3. 6 Hz seizure model

For the induction of psychomotor seizures, the mice were given corneal stimulation (6 Hz, 32 mA, 0.2 ms pulse duration, 3 s duration) (Barton et al., 2001). The corneas were treated with 1–2 drops of 0.5 % tetracaine hydrochloride about 15–20 min before electrical stimulation. The corneal electrodes were made wet with normal saline to increase the electrical conductivity to the corneas of manually held mice. The mice were immediately released after corneal stimulation (UGO BASILE rodent shocker 7801) and monitored for behavioral changes. The 6 Hz seizures are presented as animal's stunned posture with rearing, Straubing of tail, twitching of vibrissae and forelimb clonus for 60–120 s. The animals were considered protected if resumed their normal behavior within 10 s after stimulation. In the current study, each synthetic compound (100 mg/kg; i.p.) was injected 45–60 min before 6 Hz corneal stimulation. The outcomes were compared with vehicle-treated mice injected with 1 % Tween 80 (1 ml/kg; i.p.) using levetiracetam (50 mg/kg; i.p.) as standard treatment.

2.2.4. Acute PTZ test

The protection from PTZ-induced seizures is one of the primary protocols relied on to claim the antiepileptic potential of test compounds. The acute PTZ model is characterized by full body tonic/clonic seizures in rodents after the administration of the lethal dose of PTZ. The initial signs of clonic convulsions include facial and forelimb movements followed by full-body tonic-clonic seizures that eventually lead to the front and hind limb extension which is followed by the animal's death (Koutroumanidou et al., 2013).

The randomly chosen mice were divided into nine groups (*n* = 4). The animals of all groups were pre-treated with test compounds (100 mg/kg) and after 45–60 min of treatment, the animals were exposed to PTZ (80 mg/kg) (Herrera-Calderon et al., 2018) and the response was monitored for 30 min. The animals were monitored behaviorally for latency to first myoclonic twitch, latency to the episode of generalized tonic-clonic seizures, latency to seizure with hind limb extension and latency to death (Liu et al., 2019) and outcomes were compared with PTZ control animals.

2.2.5. Recording of video/EEG (vEEG) in acute PTZ test

The intraperitoneally injected ketamine/xylazine cocktail was used to anesthetize the mice (Bielefeld et al., 2017) and animals were fixed onto the stereotaxic apparatus equipped with a heating pad to circumvent the risk of hypothermia. After shaving the fur from the required area, the skin of the head was swabbed with 70 % ethanol to prepare it for aseptic surgery. The cortical screw electrodes were stereotaxically implanted at AP + 3 mm; LL \pm 1.5 mm. Additionally, one screw served as the indifferent reference electrode (AP – 2 mm; L – 1.5 mm).

m). The screw electrodes were fixed in the skull using an additional skull screw for anchoring (Bröer et al., 2016). All mounted screws and the headset were covered with dental cement. Animals were continuously monitored during the surgical procedure and were housed individually in clear polycarbonate until they recover and move freely in the cage.

After providing the 5–7 days of recovery, the individually caged mice were connected to the 8-channels bioamplifiers (ADInstruments Ltd., Sydney, Australia) and an analog–digital converter (PowerLab 8/30 ML870, ADInstruments) for EEG recording. The vEEG was recorded using a laptop equipped with a Logitech camera for video recording.

After introducing into the EEG-dedicated cages, the animals were allowed to acclimatize for 30 min. The baseline was recorded for 15–20 min and the synthetic compounds **7b** and **7c** (100 mg/kg; i.p.) were injected to separate groups of animals ($n = 4$). After an hour, the PTZ (80 mg/kg; i.p.) was administered and vEEG was recorded for 30 min using a signal sampling rate of 200 Hz and bandpass filtered between 0.1 and 60 Hz (Anjum et al., 2018). The EEGs were analyzed for electrographic alterations and spikes which were the electroencephalogram changes of at least twice the amplitude of the EEG baseline. A previously reported spike analysis algorithm by Muneeb et al. was used to analyze the spiking activity. The outcomes were expressed as the latency (*sec*) to the first post-PTZ spike and the number of spikes in 90 sec followed by the first spike (Anjum et al., 2018).

2.2.6. Molecular docking

The AutoDock Tools v1.5.6 and AutoDock v4.2 were used to carry out the molecular docking of all target compounds (Morris et al., 2009). RCSB protein data bank (<https://www.rcsb.org/>) was used for downloading the crystal structure of GABA_A-receptors (PDB ID 6HUP, co-crystallized with Diazepam (DZP)) (Berman et al., 2007). The synaptic vesicle protein 2A (SV2A) sequence was retrieved from the National Center for Biotechnology Information (NP_476558.2). Then I-Tasser server was used to convert the protein sequence (Roy et al., 2010) into 3D model of the protein. The structures of compounds were geometry/energy minimized with Chem 3D pro 12.0 and saved as a PDB file format. In the case of GABA_A receptors, the grid dimensions were calculated from an active site with the co-crystallized ligand of protein structure using Discovery Studio Visualizer version 4.0 (Waltham, MA, USA). The active site for the docking study was selected by defining a grid of dimensions 60 × 60 × 60 size with 0.375 Å over the co-crystallized ligand. For SV2A protein, the grid box was confirmed with the CB-Dock (blind docking) online tool (<https://clab.labshare.cn/cb-dock/php/>). The ligands were docked onto the SV2A protein using a 70 Å × 70 Å × 70 Å grid box which covered all putative residues involved in racetam recognition according to the literature, and a Lamarckian genetic algorithm was used for docking (Correa-Basurto et al., 2015; Shi et al., 2011). A hundred confirmations were generated and poses of the ligands were sorted based on the lowest free binding energy (Stroganov et al., 2008).

Estimated free energy of binding = [(a) + (b) + (c) – (d)].

where, (a) final intermolecular energy = vdW + dissolve energy and electrostatic energy + H-bond, (b) total internal energy, (c) torsional free energy, and (d) unbound system's

energy. The best active binding mode with the lowest energy was designated and visualized through Discovery Studio Visualizer v 4.0.

2.2.7. Data analysis

Every animal was independently observed for the parameters i.e. latency of myocolic twitch, full body generalized seizures and death which had normal distribution and evaluated by one-way ANOVA followed by Dunnett's multiple comparison test using GraphPad Prism version 8. The EEGs were analyzed with LabChart version 8 and the inter-group comparison for latency to first spike and spike counts in electroencephalogram was made by the non-parametric Mann-Whitney test. All data were expressed as Mean ± SEM considering $P < 0.05$ significant.

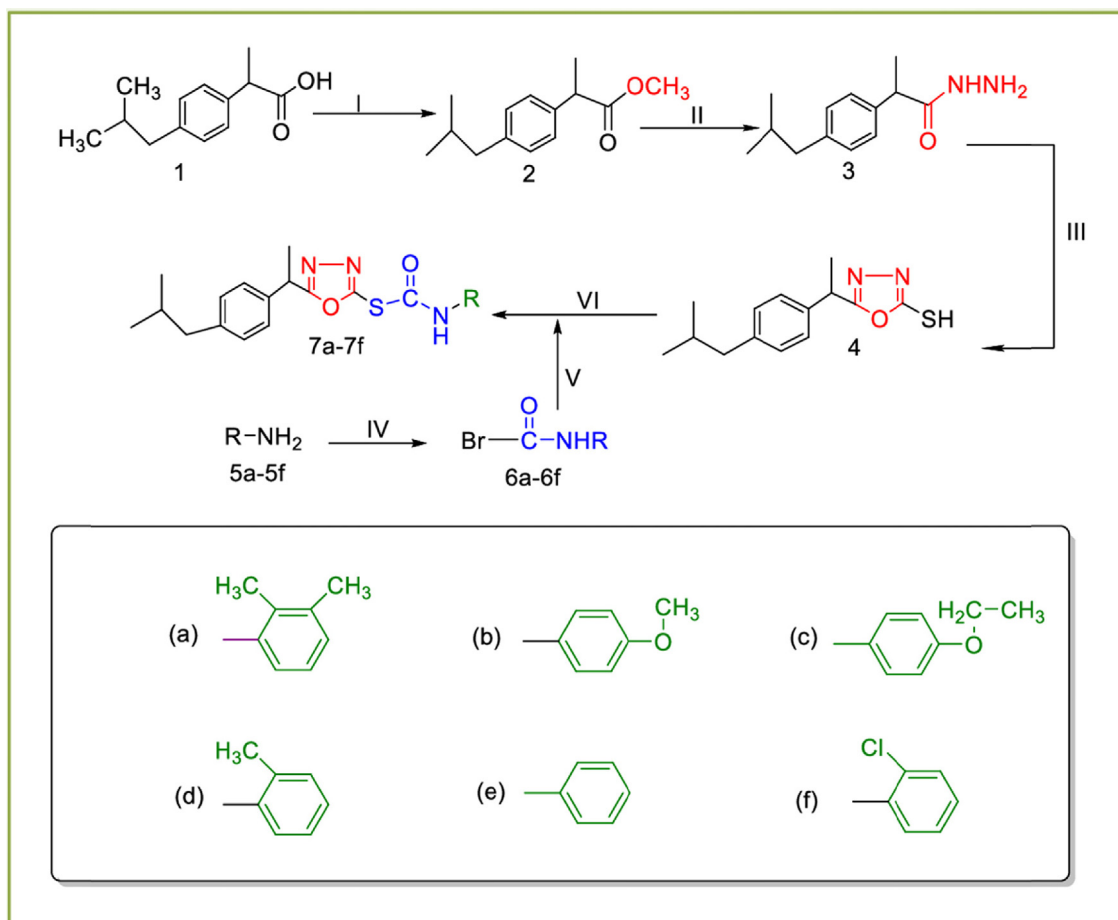
3. Results and discussion

3.1. Chemistry

Present work is a synthetic approach for the synthesis of *N*-substituted 5-aryl-1,3,4-oxadiazole-2-carbamothioate derivatives (**7a-f**) which is based upon chemical modification of 2-(4-isobutylphenyl)propanoic acid for improving their safety profile. Previously we have synthesized different oxadiazole based derivatives containing acetamide functionalities and it is proved from literature that oxadiazole possess good anti-convulsant activity So in continuation of our previous work on heterocyclic compounds (Gul et al., 2017, Khan et al., 2020, Khan et al., 2021), we have cyclized –COOH group of 2-(4-isobutylphenyl)propanoic acid into five membered heterocycle e.g.oxadiazole nucleus **4**. Oxadiazole was modified at SH by replacing its H-group with different electrophiles yielding final compounds (**7a-7f**).

The synthetic route of synthesized compounds (**7a-7f**) is in Scheme 1. Compound (**2**) was obtained by refluxing the 2-(4-isobutylphenyl)propanoic (**1**) with absolute methanol for six hour using Fischer esterification method (Gulnaz et al., 2019). The ester of 2-(4-isobutylphenyl)propanoic was gently refluxed with 80 % hydrazine hydrate (Iqbal et al., 2017) in methanol to get 2-(4-isobutylphenyl) propanehydrazide (**3**). In third step, the compound **3** was cyclized into 5-(1-(4-isobutylphenyl) ethyl)-1,3,4-oxadiazole-2-thiol (**4**) by gently refluxing the compound **3** in methanol with carbon disulfide and KOH. After completion, the reaction mixture in flask was acidified by conc. HCl and product **4** was isolated by filtration. Compound **4** was reacted with different substituted aralkyl/alkyl/aryl 2-bromocarbamides (**6a-f**) using DMF and NaH at room temperature. Reaction progress was continuously checked by TLC. After successful completion, the solvent in flask was evaporated. Chilled water was introduced in reaction mixture to get product. Product were filtered and dried. The product was also recrystallized using absolute ethanol. The structures of oxadiazole based carbamothionate derivatives were confirmed by spectroscopic (FTIR, ¹H NMR, ¹³C NMR) and physicochemical methods.

In ¹H NMR spectrum, chemical shift value for –NH proton in all derivatives was observed in between 10.10 and 9.29. The aliphatic and aromatic protons resonate between 4.35 and 0.85 ppm and 7.88–6.81 ppm respectively. Analysis of ¹H NMR spectra for compounds (**7a-7f**) exhibited the segregation



Scheme 1 Synthesis of target compounds (7a-7f): (I) $\text{H}_2\text{SO}_4/\text{EtOH}/\text{refluxing}$ for 3–4 h (II) $\text{N}_2\text{H}_4/\text{MeOH}/\text{stirring}$ for 5–6 h (III) $\text{CS}_2/\text{KOH}/\text{EtOH}/\text{refluxing}$ for 3–6 h (IV) carbonicdibromide/ $\text{H}_2\text{O}/5\% \text{Na}_2\text{CO}_3 \text{ soln.}/\text{stirring}$ for 1 h (V) $\text{DMF}/\text{NaH}/\text{stirring}$ for 2–3 h.

of peaks in four distinct regions. The protons of the aromatic ring system were the most deshielded and observed in between 7.88 and 6.81 ppm. Chemical shift value for aromatic protons of ibuprofen were observed as doublet with double integration in between 7.21 and 7.01 ppm. The aliphatic $-\text{CH}_3$ protons of ibuprofen were the most shielded one and observed around 0.86–0.84. Key evidence of formation of carbamide moiety was appearance of NH peak around 10.10–9.29 ppm. ^{13}C NMR spectroscopy also support the formation of carbamide by showing peaks at 162.15 ppm that correspond to $\text{C}=\text{O}$ group of carbamide, and peaks at 161.15 ppm corresponds to carbon nucleus of triazole ring. Characteristics signals at 22 ppm are due to two $-\text{CH}_3$ carbon nucleus of ibuprofen. Segregation of signals between 44.18 and 20.19 ppm correspond to CH_2 groups of ibuprofen. We have reported structure activity relationship by introducing some electron withdrawing substitution and compared them with electron donating group substitution on phenyl group. On the basis of medicinal importance, anticonvulsant activities of all compounds were checked.

3.2. 6 Hz

In the 6-Hz test, only two compounds out of seven compounds showed protection. The 7b and 7e protected 2/4 while 7f pro-

tected 1/4 of the animals from psychomotor seizures at pre-treatment time 1 h. However, the most prominent protection was observed in animals treated with 7c as 4/4 of the tested animals resumed the normal exploratory behaviour within 10 sec of shock application. The other two compounds were also tested at the same dose but no animals were protected. The outcomes were compared with levetiracetam (50 mg/kg), which protected 4/4 of animals (Table 1).

The 6 Hz model utilized the rectangular pulses of low frequency (6-Hz) of 0.2 ms with a current intensity of 32 mA delivered via corneal electrodes for 2–3 sec to induce seizures that mimicked psychomotor seizures occurring in human limbic epilepsy (Metcalf et al., 2017). At this low current intensity, the 6 Hz test worked as a discriminating screening tool to identify the antiseizure potential of currently synthesized compounds.

3.3. Acute PTZ test

The animals were visually monitored for behavioral changes for 30 min after PTZ injection. The one-way ANOVA revealed significant differences among all groups for all observed parameters i.e. in onset of first myoclonic twitch [$F(7,24) = 16.08, P < 0.0001$], tonic-clonic seizures [$F(7,24) = 59.17, P < 0.0001$], tonic hind limb extension [F

Table 1 The % protection in the 6 Hz psychomotor seizure model where mice (n = 4) were treated with vehicle, levetiracetam (50 mg/kg) and synthetic compounds (100 mg/kg) were given the corneal stimulation 60 min after treatment.

Group	Dose (mg/kg)	Animals tested	Animals protected	% Protection
Control	–	4	0	0 %
Levetiracetam	50 mg/kg	4	4	100 %
7a	100 mg/kg	4	0	0 %
7b	100 mg/kg	4	2	50 %
7c	100 mg/kg	4	4	100 %
7d	100 mg/kg	4	0	0 %
7e	100 mg/kg	4	2	50 %
7f	100 mg/kg	4	1	25 %

(7,24) = 18.20, $P < 0.0001$], and death [F (7,24) = 16.42, $P < 0.0001$].

The PTZ control animals showed the onset of the first myoclonic twitch within 58.00 ± 5.61 sec which was significantly delayed to 311.25 ± 42.67 ($P < 0.01$) sec in animals pretreated by **7b**. The onset of seizures remained continuous and progressed into full body tonic-clonic seizures after 87.50 ± 12.5 sec after PTZ administration. But, the administration of **7b** showed an increased latency of 518.00 ± 117.37 sec ($P < 0.01$) in the onset of tonic-clonic seizures. Unfortunately, the onset of the first myoclonic twitch and full body tonic-clonic seizures were not significantly affected by the remaining five compounds.

As the literature reports that PTZ-induced generalized tonic-clonic seizures are followed by tonic hind limb extension which causes respiratory arrest and death in rodents. In the current study, the latency to onset of tonic hind limb extension was also noted and compared among all groups. The 75 % of animals treated with **7b** did not progress to seizures with hind limb extension and remained protected from death. It was also interesting to note the significant latency of 1044.50 ± 437.76 sec to seizures with hind limb extension in **7c** treated mice. Moreover, the two out of four animals did not show the PTZ-induced hindlimb extension and death. These outcomes were significantly prominent ($P < 0.01$) as compared to PTZ

control animals where all four animals presented the seizures with hind limb extension within 203.00 ± 28.40 sec followed by death within 234.59 ± 29.07 sec (Table 2).

The PTZ provokes convulsions by antagonizing the GABA_A receptors non-competitively (Rehman et al., 2022). Gamma-aminobutyric acid type A (GABA_A) receptors are responsible for most of the fast inhibitory neuronal transmission. The balance between excitatory neurotransmission via glutamate and inhibitory neurotransmission via GABA is vital for proper neurologic function and cell membrane stability. Seizure generation and epilepsy are strongly linked with decreased levels of GABA, alterations of GABA_A receptor plasticity, trafficking, and expression (Fritschy, 2008). PTZ suppresses the transmission of inhibitory synapses, resulting in enhanced excitation of neuronal circuits. At a high dose, a single intraperitoneal injection of PTZ into an animal reliably evokes acute, severe generalized seizures (Shimada and Yamagata, 2018). Numerous studies have reported that compounds which enhance GABAergic neurotransmission and synaptosomal GABA concentration are effective in attenuating seizure severity in the PTZ seizure model (Rogawski et al., 2016).

Though the progression of epilepsy is complicated, the neuroinflammatory processes usually play a crucial role in the precipitation and exacerbation of seizures (Marchi et al., 2014).

Table 2 The assessment of the anticonvulsive potential of synthesized compounds in acute PTZ (80 mg/kg) model of mice. All data values are expressed as mean \pm SEM (n = 4) and evaluated by one-way ANOVA followed by Dunnett's test. * $P < 0.05$ denotes significant outcomes in comparison to the PTZ control group.

Group	Latency to first myoclonus twitch (sec)	Latency to tonic clonic seizures (sec)	Latency to tonic hind limb extension (sec)	Latency to death (sec)	% Protection from tonic hind limb extension	% Survival
PTZ control	58.00 ± 5.61	87.50 ± 12.5	203.00 ± 28.40	234.59 ± 29.07	0 %	0%
Diazepam	$650.00 \pm 132.28^{****}$	$1800.00 \pm 0.00^{****}$	$1800.00 \pm 0.00^{****}$	$1800.00 \pm 0.00^{****}$	100 %	100%
7a	103.50 ± 15.67	173.33 ± 31.75	462.00 ± 33.17	534.25 ± 32.40	0 %	0 %
7b	$311.25 \pm 42.67^{**}$	$518.00 \pm 117.37^{**}$	$1526.83 \pm 273.16^{****}$	$1662.50 \pm 137.50^{****}$	75 %	75 %
7c	100.50 ± 8.05	127.25 ± 7.33	$1044.50 \pm 437.76^{**}$	$1095.00 \pm 411.61^{**}$	50 %	50 %
7d	100.25 ± 8.39	334.50 ± 170.11	644.50 ± 105.27	746.50 ± 58.02	0 %	0 %
7e	109.00 ± 3.08	104.75 ± 5.07	118.00 ± 1.22	143.75 ± 13.13	0 %	0 %
7f	110.00 ± 13.08	228.25 ± 27.32	300.00 ± 25.87	392.50 ± 46.96	0 %	0 %

Besides its role as a GABA_A antagonist, PTZ administration is further linked with the up-regulation of various pro-inflammatory cytokines in the hippocampus and cerebral cortex resulting in disrupted BBB and seizure induction (Faheem et al., 2021). PTZ administration causes elevated oxidative stress and increased expression of lipid peroxidase, nitric oxide and TNF- α (Alvi et al., 2021). Normally, the COX-2 expression is significantly upregulated in hippocampal neurons within 1 h after seizures showing that neuroinflammation might be the potential therapeutic target during the treatment of epilepsy (Zhang et al., 2008).

3.4. Effects of 7b and 7c on PTZ-induced changes in EEG

The outcomes remained consistent with latency to myoclonic twitch induced by PTZ, the first epileptic spike which was two-fold of baseline appeared in PTZ control mice within 60 s of PTZ injection. These EEG changes were followed by the increased frequency of spikes in the duration of 90 sec after the first spike. The animal group pre-treated with **7b** showed a marked difference ($P < 0.05$) of duration from PTZ injection to the first epileptic spike appearance on the electroencephalogram. Evaluation of animals in terms of the number of epileptic spikes in post-first spike 90 sec found that administration of 100 mg/kg of compound **7b** significantly reduced the seizure activity as measured by the number of spikes compared to the PTZ control group (Fig. 2A and 2B). The animals treated with **7c** slightly increased the latency of the first epileptic spike from 43.75 ± 3.63 sec (PTZ control) to 52.10 ± 2.35 (7c group), the difference was not statistically significant. Similarly, the **7c** could not reduce the number of spikes in the post-first spike 90 sec (Fig. 3). It is worth mentioning that though the EEG changes were noted in all four **7c** animals

after PTZ injection, PTZ failed to induce hind limb extension and death in two of the four animals.

Oxadiazoles are compounds of synthetic origin that have been studied broadly in the last few decades (Wang et al., 2020). Their anti-inflammatory (Akhter et al., 2009), analgesic (Kaur et al., 2019) and anti-oxidant (Mihailović et al., 2017) potential have been widely reported. In preclinical studies, the administration of oxadiazole-derived compound resulted in the correction of the post-PTZ behavioural deficit by reducing the seizure's duration and delaying the seizure onset.

Ibuprofen is a widely used anti-inflammatory drug that mediates its major pharmacological effects through the inhibition of COX-2. A previous study by Liu et al reported that expression of COX-2 was reduced in rats pretreated with ibuprofen as compared to PTZ control animals (Liu et al., 2020). Our current results suggested that **7b** and **7c** worked fairly well in PTZ model. The EEG epileptiform activity, the number of epileptic spikes and overall mortality in PTZ-treated mice were reduced in **7b** treated animals. These findings are in-line with the previously reported literature where seizure latency was increased and duration as well as frequency were decreased by the anti-inflammatory drug, ibuprofen (Liu et al., 2020).

3.5. Docking studies

Epilepsy is a neurological disease that characterized by recurrent seizures. This disease originates due to abnormal electrical discharge from the brain neurons and it affects almost 1 % of the world's population. The invention of new targeted anticonvulsant drugs provides a very effective approach in epilepsy treatment. The γ -Aminobutyric acid type A (GABA_A) receptors are very crucial targets of the central nervous system drugs

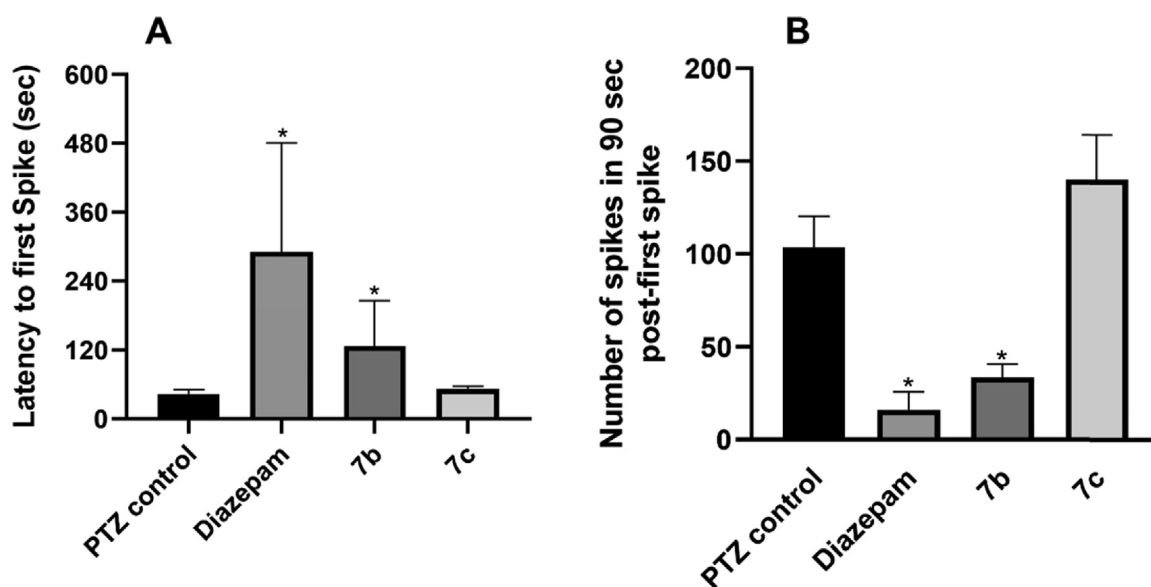


Fig. 2 After 45–60 min of pretreatment with Diazepam, **7b** and **7c** to the respective groups ($n = 4$), the animals were injected with PTZ (80 mg/kg) and (A) latency to the first epileptic spike and (B) the number of spikes in post-first spike 90sec were monitored with EEG. The PTZ control animals exhibited showed reduced latency and increased number of epileptic spikes in comparison to Diazepam and **7b** treated animals and outcomes were statistically significant when compared with the non-parametric Mann-Whitney test. All data are represented as Mean \pm SEM and * indicates significance at $p < 0.05$.

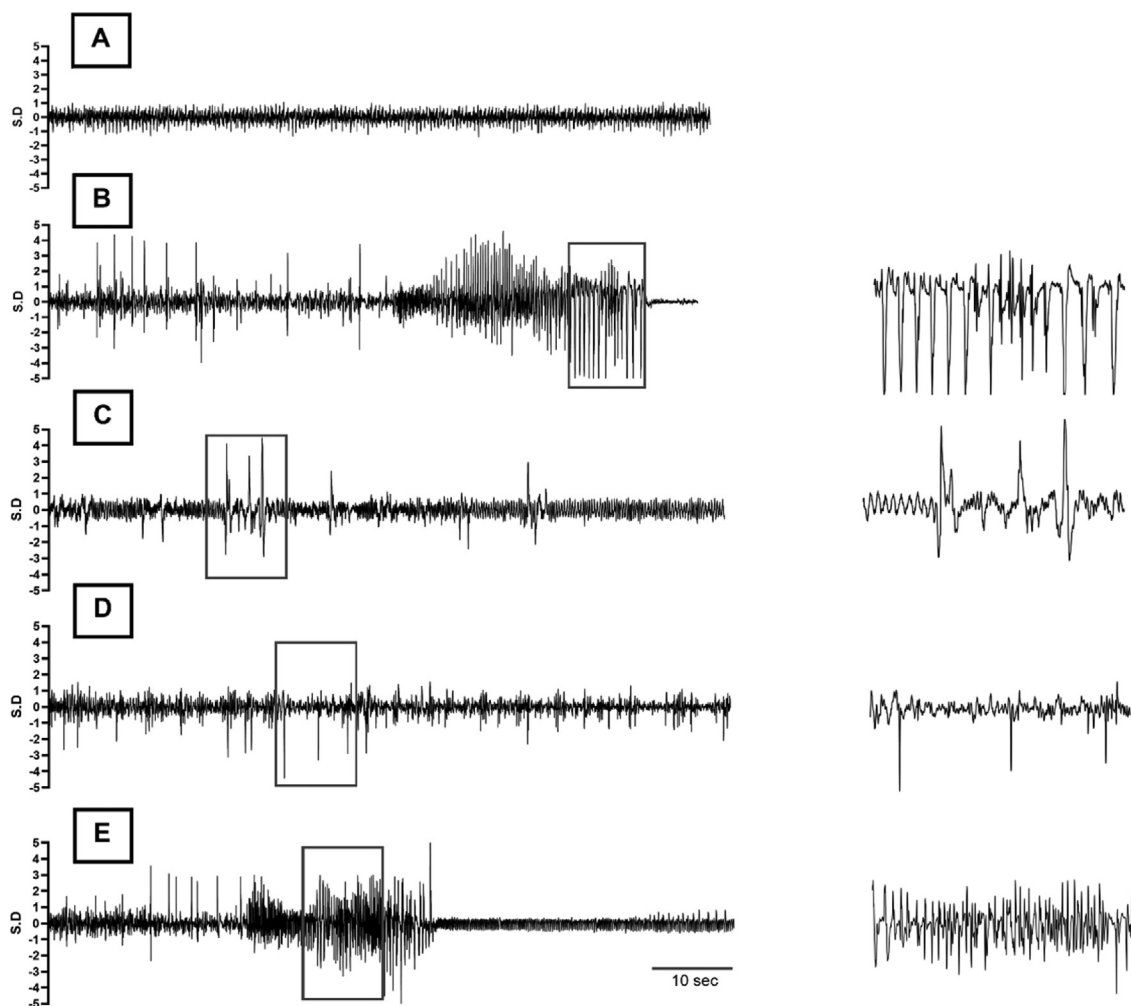


Fig. 3 Typical EEG traces recorded during the experiment. (A) Representative portion of baseline EEG before administration of the chemo-convulsant. (B-E) 90 s of electrical activity recorded after appearance of first epileptic spike post-PTZ injection, showing EEG of (B) PTZ control (PTZ only), (C) Standard Control (Diazepam + PTZ), (D) Treatment group 1 (Compound **7b** + PTZ) and (E) Treatment group 2 (Compound **7c** + PTZ), respectively. A high timed resolution of spike cluster(s) (square boxes) is shown in parallel to the corresponding EEG tracings as well.

and benzodiazepine sites on the GABA_A receptor are important active sites for the development of anticonvulsant drugs (Rudolph and Knoflach, 2011). The synaptic vesicle protein 2A is an essential membrane protein that present on all synaptic vesicles and responsible for many important functions in the central nervous system. Moreover, scientist also found out that the reduction of SV2A protein contributes in progression of epilepsy. Synaptic vesical protein 2A is the molecular target of the second-generation antiepileptic drug such as levetiracetam and its structural analogs brivaracetam and seletracetam. In recent years, molecular docking has become an important technology in the field of computer aided drug study. Therefore, an *in-silico* study was performed to identify the binding modes of the synthesized compounds with receptor proteins.

In the crystal structure of SV2A, the co-crystallized ligand is not present, therefore, the antiepileptic drug such as levetiracetam (LEV) was docked inside the SV2A protein. The docking score of the reference drug was -4.34 Kcal/mol and showed hydrogen bonding interactions with important resi-

dues Asn579, Gly687, Asn690, Ala691 and Lys694 in green color. LEV exhibited alkyl interactions with Lys580, Cys583 and Leu585 (Fig. 4A). All compounds were docked inside SV2A protein and only compounds **7b** and **7c** showed good results their binding energies are presented in Table 3. These compounds showed numerous interactions with residues such as hydrogen bonding, π -alkyl, π -stacking, and π -sulfur interactions and their bonding distance also presented in corresponding docking diagrams. Compound IOZ 3 showed better activity with its comparatively lower binding energy of -3.68 Kcal/mol. In SV2A compound **7b** forms hydrogen bonding interaction with amino acid residues Asn690 and Lys694. The π -alkyl interactions with amino acids Leu657, Ala664, and Ala691. The π -sulfur interactions are also found with amino acid residues Cys583, Cys656, and Phe686 (Fig. 4B). The **7c** also interacted with amino acid residues located at active sites of the SV2A and all possible interactions are presented (Fig. 4C). The docking study of remaining compounds is also added in supplementary data (supplementary data, S29-S30).

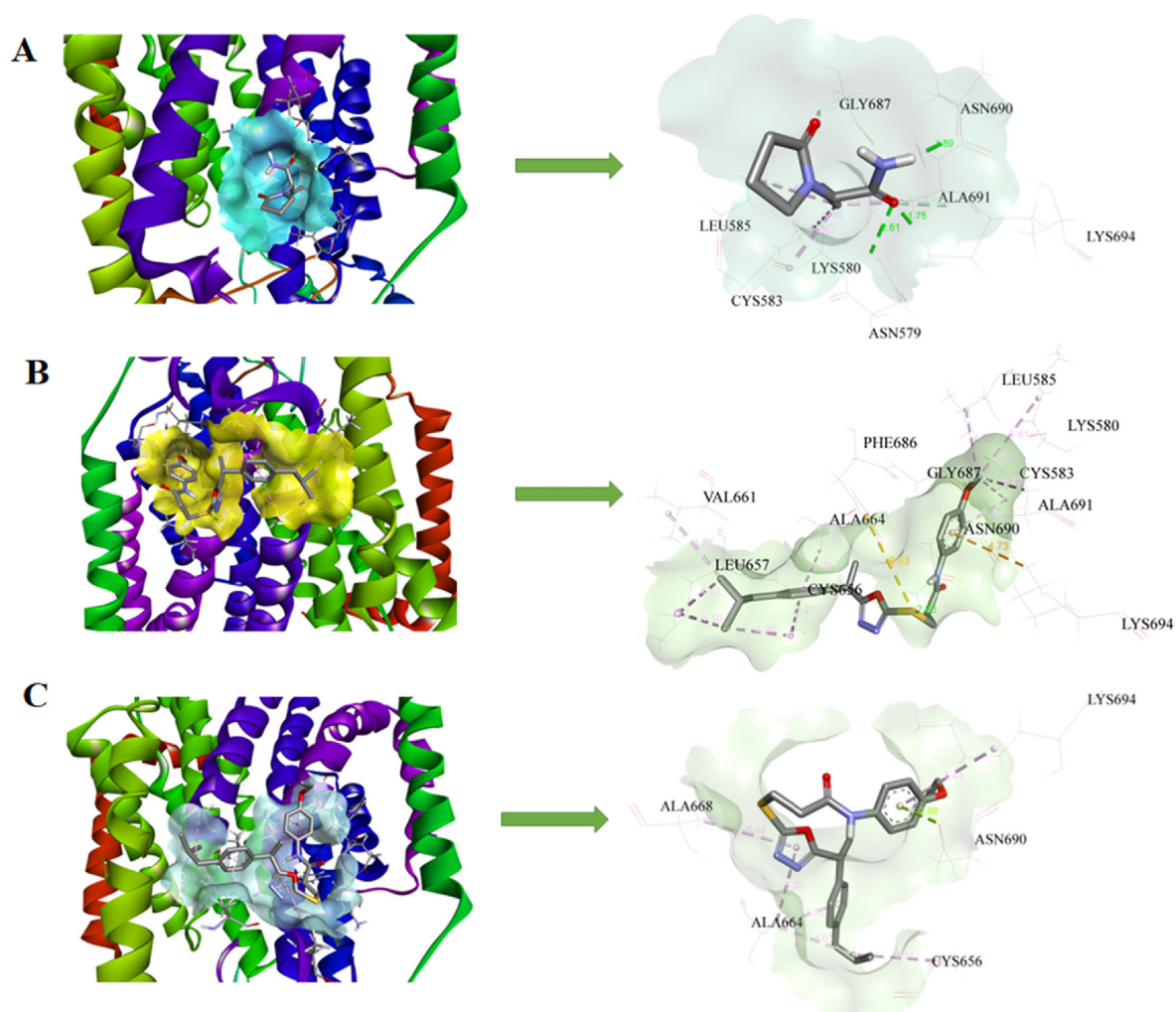


Fig. 4 3D models and schematic representations of the interactions between SV2A and (A) LEV, (B) **7b** and (C) **7c** with their bond distances. Green dashed lines represent hydrogen bonding interactions. The π -sulfur interactions are represented by yellow dashed lines. Light pink and purple lines represent π -alkyl and π - π stacked interactions respectively.

Table 3 Binding energies of target compounds (**7a-f**).

Compounds	Binding Energies against SV2A Protein (Kcal/mol)	Binding Energies against GABA _A Receptors (6HUP) (Kcal/mol)
7a	-3.55	-6.39
7b	-3.58	-6.57
7c	-3.68	-6.64
7d	-3.49	-6.29
7e	-3.38	-5.99
7f	-3.53	-6.04
Levetiracetam	-4.34	-
Diazepam	-	-6.44

The SV2A is an essential membrane protein located on all synaptic vesicles and responsible for many important functions in the central nervous system. Moreover, the scientist also found out that the reduction of SV2A protein results into the progression of epilepsy. The second-generation antiepileptic drug i.e. levetiracetam and its structural analog brivaracetam interact with this synaptic vesical protein to produce

their antiseizure effects (Lynch et al., 2008). Thus, beneficial outcomes of **7b** and **7c** compounds in 6 Hz test might be attributed to the lower binding energies and modulating the SV2A protein levels in brain.

The crystal structure of GABA_A receptors (PDB ID 6HUP, co-crystallized with Diazepam (DZP502)) was downloaded from the protein data bank. The co-crystallized ligand was

with the receptor. These observed outcomes might be attributed to the GABA_A agonistic effects of these compounds. The docking study of remaining compounds is also added in supplementary data.

4. Conclusion

Target compounds (**7a-f**) were synthesized by coupling compound (**4**) with different electrophiles under different reaction conditions, that eventually led to the synthesis of various carboxamide based oxadiazole derivatives (**7a-f**) in moderate to good yields (77–88 %). The series of compounds were tested for anticonvulsant potential in acute 6 Hz and PTZ seizure models in mice. The significantly noticeable results were observed in animals treated with **7b** and **7c**. The EEGs findings showed the reduced epileptic spiking activity in brains of **7b**-treated mice. The molecular docking studies showed that these pharmacological outcomes might be attributed to the SV2A and GABA_A modulating potentials of **7b** and **7c**, both contained electron donation groups at position 4.

Declaration of Competing Interest

The authors declare that they have no known competing financial interests or personal relationships that could have appeared to influence the work reported in this paper.

Acknowledgements

We are thankful to Mr. Muhammad Imran, an animal house attendant who is responsible for the care of animals in the animal house facility of Faculty of Pharmacy, Bahauddin Zakariya University, Multan, Pakistan.

Funding

This work was funded by Distinguished Scientist Fellowship program at King Saud University, Riyadh, Saudi Arabia through research supporting project Number (RSP2023R131).

Appendix A. Supplementary material

Supplementary data to this article can be found online at <https://doi.org/10.1016/j.arabjc.2023.104610>.

References

- Abd-Elzaher, M.M., Labib, A.A., Mousa, H.A., Moustafa, S.A., Ali, M.M., El-Rashedy, A.A., 2016. Synthesis, anticancer activity and molecular docking study of Schiff base complexes containing thiazole moiety. *Beni-Suef Univ. J. Basic Appl. Sci.* 5, 85–96.
- Ahmad, G., Rasool, N., Rizwan, K., Imran, I., Zahoor, A.F., Zubair, M., Sadiq, A., Rashid, U., 2019. Synthesis, in-vitro cholinesterase inhibition, in-vivo anticonvulsant activity and in-silico exploration of N-(4-methylpyridin-2-yl)thiophene-2-carboxamide analogs. *Bioorg. Chem.* 92, 103216.
- Akhtar, T., Hameed, S., Al-Masoudi, N.A., Khan, K.M., 2007. Synthesis and anti-HIV activity of new chiral 1, 2, 4-triazoles and 1, 3, 4-thiadiazoles. *Heteroat. Chem.* 18, 316–322.
- Akhter, M., Husain, A., Azad, B., Ajmal, M., 2009. Aroylpropionic acid based 2,5-disubstituted-1,3,4-oxadiazoles: synthesis and their

- anti-inflammatory and analgesic activities. *Eur. J. Med. Chem.* 44, 2372–2378.
- Almasirad, A., Mousavi, Z., Tajik, M., Assarzadeh, M.J., Shafiee, A., 2014. Synthesis, analgesic and anti-inflammatory activities of new methyl-imidazolyl-1,3,4-oxadiazoles and 1,2,4-triazoles. *Daru* 22, 22.
- Alvi, A.M., Shah, F.A., Muhammad, A.J., Feng, J., Li, S., 2021. 1,3,4-Oxadiazole compound A3 provides robust protection against PTZ-induced neuroinflammation and oxidative stress by regulating Nrf2-pathway. *J. Inflamm. Res.* 14, 7393–7409.
- Anjum, S.M.M., Käufer, C., Hopfengärtner, R., Walzl, I., Bröer, S., Löscher, W., 2018. Automated quantification of EEG spikes and spike clusters as a new read out in Theiler's virus mouse model of encephalitis-induced epilepsy. *Epilepsy Behav.* 88, 189–204.
- Barton, M.E., Klein, B.D., Wolf, H.H., White, H.S., 2001. Pharmacological characterization of the 6 Hz psychomotor seizure model of partial epilepsy. *Epilepsy Res.* 47, 217–227.
- Berman, H., Henrick, K., Nakamura, H., Markley, J.L., 2007. The worldwide Protein Data Bank (wwPDB): ensuring a single, uniform archive of PDB data. *Nucleic Acids Res.* 35, D301–D303.
- Bielefeld, P., Sierra, A., Encinas, J.M., Maletic-Savatic, M., Anderson, A., Fitzsimons, C.P., 2017. A standardized protocol for stereotaxic intrahippocampal administration of kainic acid combined with electroencephalographic seizure monitoring in mice. *Front. Neurosci.* 11, 160.
- Bröer, S., Käufer, C., Haist, V., Li, L., Gerhauser, I., Anjum, M., Bankstahl, M., Baumgärtner, W., Löscher, W., 2016. Brain inflammation, neurodegeneration and seizure development following picornavirus infection markedly differ among virus and mouse strains and substrains. *Exp. Neurol.* 279, 57–74.
- Chawla, G., Naaz, B., Siddiqui, A.A., 2018. Exploring 1, 3, 4-oxadiazole scaffold for anti-inflammatory and analgesic activities: a review of literature from 2005–2016. *Mini rev. Med. Chem.* 18, 216–233.
- Correa-Basurto, J., Cuevas-Hernández, R.I., Phillips-Farfán, B.V., Martínez-Archundia, M., Romo-Mancillas, A., Ramírez-Salinas, G.L., Pérez-González, Ó.A., Trujillo-Ferrara, J., Mendoza-Torrelblanca, J.G., 2015. Identification of the antiepileptic racetam binding site in the synaptic vesicle protein 2A by molecular dynamics and docking simulations. *Front. Cell. Neurosci.* 9, 125.
- Faheem, M., Althobaiti, Y.S., Khan, A.W., Ullah, A., Ali, S.H., Ilyas, U., 2021. Investigation of 1, 3, 4 Oxadiazole Derivative in PTZ-Induced Neurodegeneration: A Simulation and Molecular Approach. *J. Inflamm. Res.* 14, 5659.
- Fattorusso, A., Matricardi, S., Mencaroni, E., Dell'Isola, G.B., Di Cara, G., Striano, P., Verrotti, A., 2021. The pharmacoresistant epilepsy: an overview on existant and new emerging therapies. *Front. Neurol.* 12, 1030.
- Fritschy, J.M., 2008. Epilepsy, E/I balance and GABA_A receptor plasticity. *Front. Mol. Neurosci.* 1, 5.
- Gul, S., Abbasi, M.A., Khan, K.M., Nafeesa, K., Siddiqua, A., Akhtar, M.N., Subhani, Z., 2017. Synthesis, antimicrobial evaluation and hemolytic activity of 2-[[5-alkyl/aralkyl substituted-1, 3, 4-oxadiazol-2-yl] thio]-N-[4-(4-morpholinyl) phenyl] acetamide derivatives. *J. Saudi Chem. Soc.* 21, S425–S433.
- Gulnaz, A., Mohammed, Y.H.E., Khanum, S.A., 2019. Design, synthesis and molecular docking of benzophenone conjugated with oxadiazole sulphur bridge pyrazole pharmacophores as anti inflammatory and analgesic agents. *Bioorg. Chem.* 92, 103220.
- Herrera-Calderon, O., Santiváñez-Acosta, R., Pari-Olarte, B., Enciso-Roca, E., Campos Montes, V.M., Acevedo, L.A., 2018. Anticonvulsant effect of ethanolic extract of *Cyperus articulatus* L. leaves on pentylenetetrazol induced seizure in mice. *J. Tradit. Complement. Med.* 8, 95–99.
- Iqbal, K., Jamal, Q., Iqbal, J., Afreen, M.S., Sandhu, M.Z.A., Dar, E., Iqbal, M.M., 2017. Synthesis of N-substituted acetamide derivatives of azinane-bearing 1, 3, 4-oxadiazole nucleus and screening for antibacterial activity. *Trop. J. Pharm. Res.* 16, 429–437.

- Karaburun, A.Ç., Kaya Çavuşoğlu, B., Acar Çevik, U., Osmaniye, D., Sağlık, B.N., Levent, S., Kaplancıklı, Z.A., 2019. Synthesis and antifungal potential of some novel benzimidazole-1, 3, 4-oxadiazole compounds. *Molecules* 24, 191.
- Kaur, J., Soto-Velasquez, M., Ding, Z., Ghanbarpour, A., Lill, M.A., van Rijn, R.M., Watts, V.J., Flaherty, D.P., 2019. Optimization of a 1,3,4-oxadiazole series for inhibition of Ca²⁺/calmodulin-stimulated activity of adenylyl cyclases 1 and 8 for the treatment of chronic pain. *Eur. J. Med. Chem.* 162, 568–585.
- Khan, S.G., Bokhari, T.H., Anjum, F., Akhter, N., Rasool, S., Shah, S.A.A., Arshad, A., 2020. Synthesis, characterization, antibacterial, hemolytic and thrombolytic activity evaluation of 5-(3-chlorophenyl)-2-((N-(substituted)-2-acetamoyl) sulfanyl)-1, 3, 4-oxadiazole derivatives. *Pak. J. Pharm. Sci.* 33, 871–876.
- Khan, S.G., Naqvi, S.A.R., Ahmad, M., Akhtar, N., Bokhari, T.H., Irfan, M., Shah, S.A.A., 2021. Synthesis, spectral analysis and biological evaluation of 2-[[morpholin-4-yl] ethyl] thio-5-phenyl/aryl-1, 3, 4-oxadiazole derivatives. *Pak. J. Pharm. Sci.* 34, 441–446.
- Koutroumanidou, E., Kimbaris, A., Kortsaris, A., Bezirtzoglou, E., Polissiou, M., Charalabopoulos, K., Pagonopoulou, O., 2013. Increased seizure latency and decreased severity of pentylenetetrazol-induced seizures in mice after essential oil administration. *Epilepsy Res. Treat.* 2013, 1–6.
- Kwan, P., Brodie, M.J., 2002. Refractory epilepsy: a progressive, intractable but preventable condition? *Seizure* 11, 77–84.
- Liu, H., Wang, H., Peterson, M., Zhang, W., Hou, G., Zhang Wei, Z., 2019. N-terminal alternative splicing of GluN1 regulates the maturation of excitatory synapses and seizure susceptibility. *Proc. Natl. Acad. Sci. U. S. A.* 116, 21207–21212.
- Liu, R., Wu, S., Guo, C., Hu, Z., Peng, J., Guo, K., Zhang, X., Li, J., 2020. Ibuprofen exerts antiepileptic and neuroprotective effects in the rat model of pentylenetetrazol-induced epilepsy via the COX-2/NLRP3/IL-18 pathway. *Neurochem. Res.* 45, 2516–2526.
- Löscher, W., 2011. Critical review of current animal models of seizures and epilepsy used in the discovery and development of new antiepileptic drugs. *Seizure* 20, 359–368.
- Löscher, W., Potschka, H., Sisodiya, S.M., Vezzani, A., 2020. Drug resistance in epilepsy: clinical impact, potential mechanisms, and new innovative treatment options. *Pharmacol. Rev.* 72, 606–638.
- Löscher, W., 1999. Animal Models of Epilepsy and Epileptic Seizures in Antiepileptic Drugs. 138, 19–62.
- Lynch, B.A., Matagne, A., Brännström, A., von Euler, A., Jansson, M., Hauenberger, E., Söderhäll, J.A., 2008. Visualization of SV2A conformations in situ by the use of Protein Tomography. *Biochem. Biophys. Res. Commun.* 375, 491–495.
- Mansouri, A.-E.-E., Oubella, A., Mehdi, A., AitItto, M.Y., Zahouily, M., Morjani, H., Lazrek, H.B., 2021. Design, synthesis, biological evaluation and molecular docking of new 1, 3, 4-oxadiazole homonucleosides and their double-headed analogs as anticancer agents. *Bioorg. Chem.* 108, 104558.
- Marchi, N., Granata, T., Janigro, D., 2014. Inflammatory pathways of seizure disorders. *Trends Neurosci.* 37, 55–65.
- Metcalfe, C.S., West, P.J., Thomson, K.E., Edwards, S.F., Smith, M. D., White, H.S., Wilcox, K.S., 2017. Development and Pharmacological Characterization of the Rat 6 Hz Model of Partial Seizures. *Epilepsia* 58, 1073–1084.
- Mihailović, N., Marković, V., Matić, I.Z., Stanislavljević, N.S., Jovanović, Ž.S., Trifunović, S., Joksović, L., 2017. Synthesis and antioxidant activity of 1,3,4-oxadiazoles and their diacylhydrazine precursors derived from phenolic acids. *RSC Adv.* 7, 8550–8560.
- Morris, G.M., Ruth, H., Lindstrom, W., Sanner, M.F., Belew, R.K., Goodsell, D.S., Olson, A.J., 2009. Software news and updates AutoDock4 and AutoDockTools4: Automated docking with selective receptor flexibility. *J. Comput. Chem.* 30, 2785–2791.
- Nieoczym, D., Socala, K., Jedziniak, P., Olejnik, M., Wlaż, P., 2013. Effect of sildenafil, a selective phosphodiesterase 5 inhibitor, on the anticonvulsant action of some antiepileptic drugs in the mouse 6-Hz psychomotor seizure model. *Prog. Neuropsychopharmacol. Biol. Psychiatry* 47, 104–110.
- Obniska, J., Chlebek, I., Kamiński, K., Bojarski, A.J., Satała, G., 2012. Synthesis, anticonvulsant activity and 5-HT_{1A}/5-HT₇ receptors affinity of 1-[(4-arylpiperazin-1-yl)propyl]-succinimides. *Pharmacol. Rep.* 64, 326–335.
- Perucca, E., 2021. The pharmacological treatment of epilepsy: recent advances and future perspectives. *Acta Epileptol.* 3, 1–11.
- Rehman, Z., Farooq, T., Javaid, S., Ashraf, W., Fawad Rasool, M., Samad, N., Tariq, M., Anjum, M.M., Sivandzade, F., Alotaibi, F., Alqahtani, F., Imran, I., 2022. Combination of levetiracetam with sodium selenite prevents pentylenetetrazole-induced kindling and behavioral comorbidities in rats. *Saudi Pharm. J.* 30, 494–507.
- Rogawski, M.A., Löscher, W., Rho, J.M., 2016. Mechanisms of Action of Antiseizure Drugs and the Ketogenic Diet. *Cold Spring Harb. Perspect. Med.* 6, a022780.
- Roy, A., Kucukural, A., Zhang, Y., 2010. I-TASSER: a unified platform for automated protein structure and function prediction. *Nat. Protoc.* 5, 725–738.
- Rudolph, U., Knoflach, F., 2011. Beyond classical benzodiazepines: Novel therapeutic potential of GABA_A receptor subtypes. *Nat. Rev. Drug Discov.* 10, 685–697.
- Sharma, A.K., Rani, E., Waheed, A., Rajput, S.K., 2015. Pharmacoresistant epilepsy: a current update on non-conventional pharmacological and non-pharmacological interventions. *J. Epilepsy Res.* 5, 1–8.
- Shi, J., Anderson, D., Lynch, B.A., Castaigne, J.G., Foerch, P., Lebon, F., 2011. Combining modelling and mutagenesis studies of synaptic vesicle protein 2A to identify a series of residues involved in racetam binding. *Biochem. Soc. Trans.* 39, 1341–1347.
- Shimada, T., Yamagata, K., 2018. Pentylenetetrazole-Induced Kindling Mouse Model. *J. Vis. Exp.* 2018, 56573.
- Stroganov, O.V., Novikov, F.N., Stroylov, V.S., Kulkov, V., Chilov, G.G., 2008. Lead finder: an approach to improve accuracy of protein-ligand docking, binding energy estimation, and virtual screening. *J. Chem. Inf. Model.* 48, 2371–2385.
- Wang, S., Liu, H., Wang, X., Lei, K., Li, G., Li, J., Liu, R., Quan, Z., 2020. Synthesis of 1,3,4-oxadiazole derivatives with anticonvulsant activity and their binding to the GABA_A receptor. *Eur. J. Med. Chem.* 206, 112672.
- Xu, F.Z., Wang, Y.Y., Luo, D.X., Yu, G., Guo, S.X., Fu, H., Zhao, Y.H., Wu, J., 2018. Design, synthesis, insecticidal activity and 3D-QSR study for novel trifluoromethyl pyridine derivatives containing an 1,3,4-oxadiazole moiety. *RSC Adv* 8, 6306–6314.
- Yadav, N., Kumar, P., Chhikara, A., Chopra, M., 2017. Development of 1,3,4-oxadiazole thione based novel anticancer agents: Design, synthesis and in-vitro studies. *Biomed. Pharmacother.* 95, 721–730.
- Zaccara, G., Franciotta, D., Perucca, E., 2007. Idiosyncratic adverse reactions to antiepileptic drugs. *Epilepsia* 48, 1223–1244.
- Zarghi, A., Arfaei, S., 2011. Selective COX-2 Inhibitors: A Review of Their Structure-Activity Relationships. *Iran. J. Pharm. Res.* 10, 655.
- Zhang, H.J., Sun, R.P., Lei, G.F., Yang, L., Liu, C.X., 2008. Cyclooxygenase-2 inhibitor inhibits hippocampal synaptic reorganization in pilocarpine-induced status epilepticus rats. *J. Zhejiang Univ. Sci. B* 9, 903–915.
- Zheng, Z., Liu, Q., Kim, W., Tharmalingam, N., Fuchs, B.B., Mylonakis, E., 2018. Antimicrobial activity of 1, 3, 4-oxadiazole derivatives against planktonic cells and biofilm of *Staphylococcus aureus*. *Future Med. Chem.* 10, 283–296.
- Bala, S., Kamboj, S., Kajal, A., Saini, V., Prasad, D.N., 2014. 1,3,4-Oxadiazole Derivatives: Synthesis, Characterization, Antimicrobial Potential, and Computational Studies. *Biomed Res. Int.* 2014, 172791.
- Khan, M. ul H., Hameed, S., Akhtar, T., Al-Masoudi, N.A., Al-Masoudi, W.A., Jones, P.G., Pannecouque, C., 2016. Synthesis, crystal structure, anti-HIV, and antiproliferative activity of new oxadiazole and thiazole analogs. *Med. Chem. Res.* 25, 2399–2409.